Running title: Efficient differentiation of hepatocyte from hESCs

# Efficient Differentiation of Hepatocytes from Human Embryonic Stem Cells Exhibiting Markers Recapitulating Liver Development *In Vivo*

David C. Hay,[a,e*] Debiao Zhao,[a*] Judy Fletcher,[a,e] Zoe A. Hewitt,[a,f] Doris McLean,[b] Alai Urrutikoetxea-Uriguen,[c] James R. Black,[d] Cliff Elcombe,[b] James A. Ross,[d] C. Roland Wolf,[b] Wei Cui [a,c]

[a] Department of Gene Function and Development, Roslin Institute, Roslin, Midlothian, EH25 9PS, UK; [b] CXR Biosciences Ltd**.** James Lindsay Place, Dundee, DD1 5JJ, UK; [c] Institute of Reproductive and Developmental Biology, Imperial College London, Du Cane Rd, London W12 ONN UK. [d] Tissue Injury and Repair Group, Chancellor's Building, University of Edinburgh, Edinburgh EH16 4SB, UK;

*Authors contributed equally to this work

Current address: [e]Centre for Regenerative Medicine, Chancellor's Building, University of Edinburgh, Edinburgh EH16 4SB, UK; [f]Centre for Stem Cell Biology, The University of Sheffield, Alfred Denny Building, Sheffield, S10 2TN, UK.

Correspondence: Wei Cui, PhD, Institute of Reproductive and Developmental Biology, Imperial College London, Du Cane Rd, London W12 ONN UK.
Tel: +44-(0)20 7594 2124; Fax: +44-(0)20 7594 2154; Email: wei.cui@imperial.ac.uk

Key words: hepatocyte differentiation, human embryonic stem cell, cytochrome P450, liver development.

**ABSTRACT**

The potential to differentiate human embryonic stem cells (hESCs) *in vitro* to provide an unlimited source of human hepatocytes for use in biomedical research, drug discovery and the treatment of liver diseases holds great promise. Here we describe a three-stage process for the efficient and reproducible differentiation of hESCs to hepatocytes by priming hESCs towards definitive endoderm with Activin A and Sodium Butyrate prior to further differentiation to hepatocytes with dimethyl sulfoxide (DMSO) followed by maturation with hepatocyte growth factor (HGF) and oncostatin M. We have demonstrated that differentiation of hESCs in this process recapitulates liver development *in vivo*: following initial differentiation, hESCs transiently express characteristic markers of the primitive streak mesendoderm before turning to the markers of the definitive endoderm; with further differentiation, expression of hepatocyte progenitor cell markers and mature hepatocytes markers emerged sequentially. Furthermore, we have provided evidence that the hESC-derived hepatocytes are able to carry out a range of hepatocyte functions: storage of glycogen, generation and secretion of plasma proteins. More importantly, the hESC-derived hepatocytes express several members of cytochrome P450 isozymes and these P450 isozymes are capable of converting the substrates to metabolites and respond to the chemical stimulation. Our results have provide evidence that hESCs can be differentiated efficiently *in vitro* to functional hepatocytes, which maybe useful as a *in vitro* system for toxicity screening in drug discovery.

## INTRODUCTION

Human embryonic stem cells (hESCs) are able to replicate indefinitely and to differentiate into most, if not all, cell types of the body, thereby having the potential to provide an unlimited source of cells for a variety of applications. These include regenerative medicine for a broad spectrum of human diseases, elucidating mechanisms underlying cell fate specification and as *in vitro* models for determining the metabolic and toxicological properties of drug compounds [1, 2]. Many of these applications require efficient and regulated differentiation of hESCs to specific cell types. Hepatocytes, the primary cells of the liver, have attracted particular attention as the liver plays a central role in multiple functions of the human body and liver failure is often only treatable by liver transplantation. Unfortunately, the number of donors is insufficient to cope with the growing demand for transplantation. Hepatocyte transplantation, to increase the number of functional hepatocytes, could be employed as an alternative therapeutic approach to whole organ transplantation for liver failure. Stem cell-derived hepatocytes could also be utilised for extra-corporeal support devices in the case of acute liver failure [3]. In addition to their therapeutic potential, human hepatocytes are valuable for assessing the toxicity of new drugs, as liver is the primary tissue involved in the metabolism of drug compounds and is among the most common tissues affected by drug toxicities. Primary human hepatocytes suffer from not only inconsistent availability but also significant phenotypic and genotypic variability. Although animal models have wide application in preclinical drug development they are often not predictive for man.

Several studies have reported the differentiation of hepatocyte-like cells from human embryonic stem cells [4-6]. However, these papers have mainly focused on characterizing the final hESC-derived hepatocytes and lack of evidence that hepatocyte differentiation followed the liver developmental process *in vivo*. The liver, similar to the pancreas, develops from the primitive gut tube which is formed by a flat sheet of cells, called definitive endoderm [5, 7]. Definitive endoderm is one of the three germ layers derived from the epiblast of the inner cell mass of the blastocyst and is generated during the gastrulation stage of embryogenesis. During gastrulation, cells from specific regions of the epiblast are recruited to form the primitive streak where they transform and give rise to both mesoderm and definitive endoderm [8, 9]. The definitive endoderm at the anterior ventral segment of the gut tube interacting with cardiogenic mesoderm becomes more proliferative and forms the liver bud where cells are referred to as hepatoblasts [10, 11]. The hepatoblasts proceed through a series of maturation steps which accompany autonomous proliferation, cellular enlargement and functional maturation as the liver develops. During this process, cells express certain characteristic genes which represent cellular development with the primitive streak and definitive markers at early developmental stages being replaced by hepatic markers at later stages.

After the emergence of the liver bud from the developing gut tube, the level of hepatic maturation is characterized by the expression of liver- and stage-specific genes [12]. For example, alpha-fetoprotein (AFP) is an early hepatic marker, expressed by hepatoblasts in the liver bud until birth, when expression is dramatically reduced [13]. In contrast, albumin, the most abundant protein synthesized by hepatocytes, is initially expressed at lower levels in early fetal hepatocytes but this increases as the

hepatocytes mature, reaching a maximum in adult hepatocytes [14]. Furthermore, isoforms of cytochrome P450s (CYPs) proteins also exhibit differential expression levels according to developmental stages of the liver. CYP3A7 is mainly expressed in human fetal liver while CYP3A4 is the predominant isoform in adult hepatocytes [15].

Previously we developed a method to differentiate hESCs to hepatocyte-like cells [16]. In the present study, we have improved the procedure further and have significantly increased hepatocyte production from hESCs. We show that by priming hESCs to differentiate through the primitive streak mesendoderm to definitive endoderm prior to treatment with DMSO increases the proportion of hepatocytes in the end population to approximately 70%. Furthermore, we show that the gene expression profile during this differentiation process recapitulates that of *in vivo* development and the derived hepatocytes performed multiple liver functions.

## MATERIALS AND METHODS

### Cell culture and differentiation

Human embryonic stem cells H1 and H7 were cultured and propagated in matrigel coated plates with mouse embryonic fibroblast conditioned medium (MEF-CM) supplemented with basic fibroblast growth factor in feeder-free, serum-free conditions as previously described [17-19].

The differentiation was initiated, when hESCs reached a confluence level of approximately 50-70%, by replacing the MEF-CM with priming medium A (RPMI1640 containing 1x B27 (both from Invitrogen), 1mM sodium butyrate (NaB,

Sigma) and 100ng/ml activin A (PeproTech)). After 24-48 hours, the medium was changed to priming medium B which is the same as priming medium A, except the concentration of sodium butyrate was reduced to 0.5mM and cells were cultured for a further 48-72 hours. The cells were then split 1:2 to new matrigel coated plates and cultured in differentiation medium (SR/DMSO medium: knockout-DMEM containing 20% serum replacement (SR), 1mM glutamine, 1% non-essential amino acids, 0.1mM β-mercaptoethanol (all from Invitrogen) and 1% dimethyl sulfoxide (DMSO, Sigma)), for 7 days. Finally, the cells were cultured in maturation medium (CL15 medium [20]: L15 medium supplemented with 8.3% fetal bovine serum, 8.3% tryptose phosphate broth, 10μM Hydrocortisone 21-hemisuccinate, 1μM insulin (all from Sigma) and 2mM glutamine) containing 10ng/ml hepatocyte growth factor (HGF) and 20ng/ml oncostatin M (both from R&D systems). The medium was changed daily during differentiation.

**RNA isolation and reverse transcription–polymerase chain reaction**

Total RNA was isolated using RNeasy mini kit (Qiagen) following manufacturer's instruction and DNA was removed by the treatment with DNase (Qiagen). cDNA was synthesised using 2μg total RNA with reverse transcriptase (Roche) in a 20-25μl volume. PCR was carried out as previously described [21]. Primer sequences and PCR conditions are provided in supplemental data Table 1.

**Immunoblotting, immunocytochemistry and flow cytometry**

Cells were lysed and sonicated in sodium dodecyl sulphate (SDS) buffer and the lysates were separated in 8% polyacrylamide gels containing SDS, then transferred to nitrocellulose membrane. Western blotting was carried out as previously described

[16]. For immunostaining, cells were fixed in 4% paraformaldehyde for 10 minutes at room temperature and washed with PBS. After blocking with PBS containing 10% goat serum, cells were incubated with primary antibody at 4°C overnight, followed by 30 minutes incubation with appropriate secondary antibody at room temperature. The primary and secondary antibodies used are commercially available except CYP3A and CYP2D6 which are from Prof. R. Wolf's laboratory. For flow cytometry, cells were harvested and incubated in blocking buffer containing 40% goat serum for 30 minutes followed by incubation with CXCR4-PE antibody following manufacturer's instruction. The cells were analysed in Beckon Dickinson flow cytometer after washing. All the antibodies and conditions are listed in supplemental data Table 2. The controls were performed by replacing the primary antibodies with corresponding IgG antibodies and they were negative. The counting on albumin and Hepar 1 staining were done on 300-400 cells in 4 random chosen fields.

**Measurement of hepatocyte export proteins**

Cells were cultured in 6-well plate in 3ml appropriate media and after 24 hours supernatants were collected for export protein assay. The hepatic export proteins alpha-2-macroglobulin (A2M), haptoglobin, fibrinogen and fibronectin were measured using sandwich enzyme-linked immunosorbent assays (ELISA) essentially as described by the manufacturer (DAKO, Ely, UK). High binding EIA plates (Corning, Koolhovenlann, Netherlands) were coated with rabbit anti-human antibody (DAKO, Ely, UK) to each specific protein overnight at 4°C. Antibodies were diluted 1:1000 for A2M and fibronectin, 1:2000 for haptoglobin and 1:10000 for fibrinogen. Sample supernatants were diluted 1:10 and then added to 96-well plate in triplicates. The plates were incubated for 2 hours at room temperature. Peroxidase-conjugated

rabbit anti-human antibody (DAKO) directed against the appropriate protein was added and the plates were incubated for 1 hour at room temperature. The substrate o-phenylenediamine (OPD) was added and the reaction stopped with 0.5M sulphuric acid. The plates were read at 490 nm with a reference wavelength of 630nm using a MRX II plate reader (Dynatech, Billinghurst, UK) and the concentration of the appropriate protein in each sample was calculated from standard curves using the MRX II Endpoint software. Analysis of significance between variables was performed using the paired two-tailed t-test. A difference was considered significant using 95% confidence intervals ($P<0.05$).

**Measurement of basal metabolism**

hESC-derived hepatocytes and HepG2 cells (ECACC no 85011430) were incubated with a cocktail of midazolam, bufuralol, phenacetin and tolbutamide, each at a final concentration of 10µM except tolbutamide which was at 100µM in the culture medium. After 24 hours, medium was collected and treated with acetonitrile to prevent further enzyme activity. The concentration of the metabolites, 1'-hydroxymidazolam, 1'-hydroxybufuralol, acetaminophen and 4'hydroxytolbutamide, were measured using reverse phase HPLC with tandem mass spectrometric detection (LC-MS/MS) and the amounts were calculated according to the standards which were prepared 0-500ng/ml in the same culture medium. All the P450 substrates and metabolites were obtained from Ultrafine Chemicals or Sigma-Aldrich. The metabolites were normalised over alanine aminotransferase (ALT) activity which was measured from cell lysates using a Cobas Integra 400 clinical analyzer (Roche) and an *in vitro* diagnostic reagent system for ALT.

### CYP3A4 induction

Triplicate T25 flasks of hESC-derived hepatocytes as well as HepG2 cells were treated with rifampicin at a final concentration of 25μM or DMSO for 72 hours. The rifampicin-containing medium was replaced with medium containing CYP3A4 substrate midazolam at concentration of 10μM. After 24 hours, medium was collected and 1'-hydroxymidazolam metabolite was measured with LC-MS/MS as described above.

## RESULTS

### Directed hepatocyte differentiation from hESCs

We have developed a three-step protocol by modifying our previous method [16] to maximize hepatocyte production from hESCs (Fig.1A and Methods). In this protocol, hESCs, routinely cultured without feeder cells as described previously [18], were first treated with 100ng/ml activin A and 1 mM NaB for 24-48 hours, followed by 2-3 days of 100ng/ml activin A and 0.5 mM NaB. During the first 24-hour period, we observed dramatic cell death, the surviving cells proliferated well, reaching about 70% confluence by the end of the priming stage (Fig.1A). The cells were then split at a 1:2 ratio and cultured in unconditioned ES medium supplemented with 1% DMSO for 7 days. The cells gradually exhibited morphological change from a spiky shape to a polygonal outline (Fig. 1B). Finally, the medium was changed to modified L15 medium (see Methods for details) supplemented with 10ng/ml hepatocyte growth factor (HGF) and 20ng/ml oncostatin M (OSM) for a further 7 days. During the differentiation process, the hESCs went through a series of profound morphological

changes and hepatocyte morphology started emerging from day 9. By day 13, the cells revealed characteristic hepatocyte morphology: polygonal in shape and distinct round nuclei (Fig. 1B & Suppl. Fig.7A).

Direct comparison of this protocol with the previous one showed that the priming protocol significantly increased the production of hepatocyte-like cells from about 10% to 70%. The percentage of hepatocytes differentiated from hES cells using this protocol was estimated at 71% (± 7.5%) of all cells by counting albumin positive cells and 65% (±7.1%) of all cells by counting hepatocyte specific marker, Hepar1 positive cells at day 17 of differentiation. The remaining 30% cells were mainly fibroblast-like cells. The hESC-derived hepatocytes could be maintained in the final stage culture conditions for up to 5 days after characteristic hepatocyte morphology appeared, after which they began to deteriorate with increasing numbers of fibre-like cells (Suppl. Fig. 7B). The time taken for the hES cell-derived hepatocytes to deteriorate in culture is very similar to that observed for primary human hepatocytes.

**Gene expression pattern during differentiation from hESCs to hepatocytes reflects the progress of liver development *in vivo*.**

Gene expression analysis showed that the expression of genes during the differentiation process of hESCs recapitulated that of the liver developmental process *in vivo* (Fig.2A-C and suppl Fig.8). In the first priming stage of differentiation, hESCs were transitioned through mesendoderm to definitive endoderm. This is represented by transient upregulation of brachyury, the gene expressed by the primitive streak mesendoderm and downregulated in definitive endoderm; persistent expression of goosecoid (GSC), CXCR4 and hepatocyte nuclear factor 3 beta (FoxA2), genes which

are expressed by the primitive streak but continuously expressed by the definitive endoderm progenitors [8, 22]; and increased expression of Sox17, a definitive endoderm marker. Following transfer to SR/DMSO medium in stage 2 of differentiation, hepatocyte nuclear factor 4α (HNF4α), 1α (HNF1α) and 1β (HNF1β) were dramatically upregulated, followed by increased expression of transthyretin (TTR) which is controlled by HNF4α [23]. Towards the end of stage 2, high expression of α-fetoprotein was evident, indicating hepatoblast or early hepatocyte formation [24]. By stage 3, expression of albumin, the most abundant protein in the liver, was significantly increased and maintained. Other proteins related to liver functions were also expressed at this stage, such as apolipoprotein F (ApoF), constitutive androstane receptor (CAR) and tryptophan dioxygenase (TO). Up-regulation of tyrosine aminotransferase (TAT) and CYP7A1 (Suppl. Fig. 9) in the hESC-derived hepatocytes indicates the hESCs were differentiated to heptic cell fate rather than yolk sac cells [25]. There was no clear Pax6 expression after the differentiation, indicating no neural ectoderm differentiated.

The gene expression pattern was further analysed by western blot. The results of western blotting (Fig. 2B) confirmed the progression of gene expression detected by RT-PCR. Oct4 protein was considerably downregulated after 1 day differentiation and became undetectable at stage 2 of the differentiation. FoxA2 was clearly upregulated early around day 2 of differentiation and HNF4α was present at high levels from day 5 of stage 2. The early hepatocyte gene, AFP, appeared near the end of stage 2 and the more mature marker albumin was expressed at the beginning of stage 3. By stage 3, the hepatocyte-like cells also expressed increasing levels of c-met, the HGF receptor. In general, expression of mRNAs and proteins showed same pattern. The subtle

differences between RT-PCR and western blot on HNF4α and albumin mainly reflect sensitivity difference between the two techniques.

Immunostaining further confirmed the specificity of gene expression. During stage 1 differentiation, CXCR4 expressing cells increased significantly from less than 15% before differentiation to over 70% at end of stage 1, which is similar as reported (Fig. 2D) [26]. The transcription factors FoxA2 and HNF4α were localised in the nuclei, and AFP, albumin, and hepar1 showed cytoplasmic staining (Fig. 3A). The hESC-derived hepatocytes were also stained positive for aminopeptidase N (CD13) which has been reported to be positive for canaculi [27]. When stained with cytokeratin antibodies, CK18 and CK19, most of the hESC-derived hepatocytes were positive (Fig. 3B).

**Activin A and sodium butyrate co-operate to increase hepatocyte production from hESCs**

In our previous method, we applied the SR/DMSO directly on hESCs to induce differentiation [16]. The resulting hepatocytes exhibited typical polygonal morphology and performed a range of hepatocyte functions. However, the percentage of hepatocytes in the population was low, with approximately 10% of the cells developing hepatocyte morphology, the rest of the cells were of mixed cell types, indicating that differentiation induced by DMSO is not lineage-specific. We proposed that priming hESC differentiation to definitive endoderm prior to DMSO treatment would be crucial in leading to more efficient hepatocyte differentiation. Increasing evidence show that activin/nodal signalling pathway are important for definitive endoderm differentiation [28-30]. Sodium butyrate (NaB) has been reported to

contribute to more homogeneous hepatocyte differentiation [4] and more recently, NaB and activin A together are found to induce definitive endoderm differentiation from hESCs [31] . In order to further investigate the role of activin A and NaB in the definitive endoderm differentiation, the hESCs (both H7 and H1) were treated with activin A or NaB alone or with both. After the first 24 hours of treatment, the later two conditions displayed substantial levels of cell death. Therefore, the NaB was reduced to 0.5mM for a further two days before replaced by DMSO containing medium. At this point, the cells from all of these treatments displayed similar morphologies. However, after 4 days culture in DMSO containing medium, the cells exhibited different changes in morphology. A considerable number of the cells in activin/NaB combined treatment had revealed early hepatocyte morphology, while cells treated with activin alone resulted in less hepatocyte formation and no clear hepatocyte differentiation was observed in NaB treatment (Fig. 4A).

The profile of gene expression was analysed throughout the first three days and was very similar between the combined and activin alone treatments, but different from NaB treatment (Fig. 4B). The former showed primitive streak and definitive endoderm markers expression, such as mixL1 GSC, Sox17 and FoxA2, which are very low or absent in NaB alone treated cells. However, the undifferentiation marker gene nanog had obvious higher expression in activin alone treated cells than those treated with combined activin and NaB, indicating that in the current conditions activin alone treatment for 3 days contained more undifferentiated cells which may result in more heterogeneous population after further differentiation with DMSO.

**Liver function in hESC-derived hepatocytes**

To test the functionality of hESC-derived hepatocytes, we carried out several experiments. One of the functions of the liver is its production and export of plasma proteins which are important in maintaining homeostasis of the body. In addition to albumin, other proteins include fibrinogen, a zymogen of fibrin which is important for blood clotting function; fibronectin, an important extracellular protein capable of binding receptor proteins, and alpha-2 macroglobulin (A2M), a multifunctional binding protein. To examine if the hESC-derived hepatocytes were capable of synthesizing and releasing these proteins into the culture medium, we measured these proteins in the culture medium by enzyme-linked immnosorbent assay (ELISA) during the stage 3 when early hepatocytes had formed. The data clearly show that these export proteins were significantly increased in the culture medium in comparison with hESC controls and the production of these proteins peaked at the later stages of the differentiation protocol when the hESC-derived hepatocytes were more mature (Fig. 5A).

Another important function of liver is metabolism and detoxification, in which P450 cytochrome enzymes (CYPs) play a critical role. Thus, we examined expression of several members of this multigene family, including CYP3A4, CYP3A7, CYP2D6, CYP2C9 and CYP2C19 in the hESC-derived hepatocytes either by RT-PCR or western blotting. The western blotting results showed a marked increase in the expression of CYP3A and CYP2D6 proteins after hESCs were differentiated to hepatocytes (Fig. 6A). The CYP3A expression was also detected by immunostaining (Fig. 5B). The RT-PCR showed that both CYP3A4 and CYP3A7 were expressed in hESC-derived hepatocytes and the specificity and fidelity of CYP3A4 and CYP3A7 PCR products was confirmed by sequencing (Fig. 6B). The expression levels of

CYP3A4 in the hESC-derived hepatocytes was similar to that observed in fetal liver tissues but lower than in adult liver and the CYP3A7 expression was lower than in fetal tissues. We also detected CYP2C9 and CYP2C19 expression in the hESC-derived hepatocytes though the levels were lower than in adult liver tissues. In addition to the P450 isozymes, the expression of the cytochrome P450 reductase (CPR), an important redox partner for all CYPs, and expression of pregnane X receptor (PXR) and constitutive androstane receptor (CAR), nuclear receptors important for the transcriptional regulation of P450s and other drug metabolising enzymes [32] (particularly CYP3A4 and CYP2B6) in the presence of foreign toxic substances, were clearly induced in the hESC-derived hepatocytes after differentiation (Figs. 5B, 2A and 6B respectively).

To determine the activity of P450 isozymes, we measured the metabolism of the P450 substrates midazolam, tolbutamide, bufuralol and phenacetin by measuring the formation of their metabolites after 24 hours. CYP3A4 metabolises midazolam to 1'hydroxymidazolam while the metabolism of tolbutamide to 4'hydroxytolbutamide is catalysed by CYP2C9. Phenacetin is converted to acetaminophen by CYP1A2 or CYP2E1 and bufuralol is metabolized to 1'hydroxybufuralol by CYP2D6. The metabolites of all substrates were detected in hESC-derived hepatocytes (Fig, 6C), which demonstrated that the P450 isozymes expressed in these cells are active. When compared to the most commonly used human hepatocyte cell line, HepG2, the hESC-derived hepatocytes showed considerably higher rates of metabolism of midazolam and tolbutamide. The tolbutamide metabolism was not detected in HepG2 cells. We further tested the induction of CYP3A4 upon chemical stimulation since it is the most prevalent P450 isozyme in adult liver and is involved in the metabolism of a

significant proportion of currently used drugs [33]. Since the human form of CYP3A4 can be induced with rifampicin through the transcription factor PXR, we treated both hESC-derived hepatocytes and HepG2 cells with rifampicin for 72 hours followed by treatment with CYP3A4 substrate, midazolam, and the formation of 1'hydroxymidazolam was measured by mass spectrometry. hESC-derived hepatocytes produced higher levels of metabolites in response to rifampicin treatment although the increase was less than 2 fold (Fig. 6D). This suggests that the hESC-derived hepatocytes do respond to chemical treatment and that PXR is active in these cells.

We also examined the glycogen storage function in the hESC-derived hepatocytes using Periodic Acid Schiff (PAS) staining. In compare with fibroblast (Suppl. Fig. 7B), the hESC-derived hepatocytes exhibited evident glycogen storage (Fig.5B).

## DISCUSSION

We have developed a new differentiation protocol based on our previous one for efficient differentiation of hepatocytes from human ES cells. Direct comparison of the two protocols showed that activin priming protocol exhibited significant increase in the number of hepatocyte-like cells (70%) in compare with the previous protocol (10%) though hepatocytes derived from both protocols showed similar gene expression pattern (Fig. 2 and [16]). However, due to the low efficiency, we were unable to carry more detailed analysis on previous differentiation as we had to dissect hepatocyte foci for RT-PCR. With current protocol, we were able to extract RNA and protein from whole cell population and performed gene expression analysis during the

differentiation. The results indicated that gene expression in the current *in vitro* differentiation process from ES cells to hepatocytes recapitulates liver development *in vivo*. This in vitro model, therefore, will be useful for future studies to elucidate molecular mechanisms regulating hepatocyte differentiation/liver development. In stage 1, the hESCs first converted to cells similar to the primitive streak mesendoderm cells, then to the cells resembling those in the definitive endoderm. This was characterised by the gradual downregulation of undifferentiated gene expression, such as Oct4 and nanog, transient increase of brachyury expression and upregulation of GSC, Sox17 and FoxA2 expression. During stage 2 of differentiation, the definitive endoderm cells further differentiated to hepatocyte progenitor cells as shown by the gradual sequential upregulation of HNF4a, AFP and AAT. In addition, the cell morphology changed from a triangular spiky shape to the characteristic polygonal shape. Finally in the stage 3 of differentiation, the heypatocyte progenitor cells further developed into more mature hepatocytes as shown by the increasing expression of albumin, apolipoprotein F, CAR, TO and c-met receptor; evident glycogen storage and generation and secretion of plasma proteins. The cells exhibited characteristic morphology of the liver hepatocytes.

In addition, by the end of stage 3, the hESC-derived hepatocytes also expressed NADPH-cytochrome P450 oxidoreductase (CPR), several cytochrome P450s and pregnane X receptor (PXR). Moreover, not only are the P450 enzymes expressed but also they could convert substrates to metabolites more efficiently than HepG2 cells. We are interested in CYP3A family members, particularly CYP3A4 as it is critical for the drug metabolism [33]. The hESC-derived hepatocytes expressed detectable levels of both CYP3A4 and CYP3A7 and responded to rifampicin treatment. This has

important implications for the application of hESC-derived hepatocytes as an *in vitro* model for drug development. Since it is very difficult to obtain human liver tissues, we were unable to directly compare our hESC-derived hepatocytes to primary human hepatocytes on the functionality tests. However, from the gene expression analysis, we think that to be able to use hESC-derived hepatocytes for drug screening, further improvement may be required, particularly on maturation. The current protocol has significantly improved differentiation efficiency but the hESC-derived hepatocytes are probably still at fetal liver developmental stage as indicated by high expression of AFP and low expression of Cyp3A4. It remains a challenge on how to further mature hESC-derived hepatocytes. Liver development *in vivo* occurs in a 3-dimensional (3D) environment but *in vitro* culture is 2-dimensional (2D). Although this 2D system may aid efficient differentiation of hESCs to hepatocytes as cells receive more synchronous induction, the 3D culture environment promotes cell-cell interactions which may further enhance maturation and function [34, 35]. In addition, the current culture conditions may not be ideal for further hepatocytes maturation. We have changed maturation medium from hepatocyte culture medium [16] to the current modified L15 medium which has reduced appearance of vacuole-like structures in maturing hepatocytes and proliferation of non-hepatocytes, mainly fibroblasts. Further improvements of the culture conditions may help further maturation and enhance functionality. Moreover, although the majority of the cells in the liver are hepatocytes, the liver also contains other cell types, such as Kupffer cells, liver endothelial cells, etc. These cells may have an effect on hepatocyte maturation and liver function. Future work on maturation will need to take these factors into account.

In our differentiation protocol, the combination of activin A and NaB treatment primes hESCs more efficiently after further differentiation to hepatocytes than the activin A alone. However, when we checked the gene expression patterns after stage 1 in both H1 and H7 cells, the activin A only treated group seemed to have higher expression of the definitive endoderm markers (e.g. Sox17, FoxA2) and NaB itself did not show any evidence of promoting hESCs to the definitive endoderm. This raises the question of the role of NaB in this process. NaB, a short-chain fatty acid, is a histone deacetylase (HDAC) inhibitor and has been reported to induce growth arrest, differentiation and apoptosis in a number of cancer cells [36, 37]. Since NaB and the combined treatment resulted in more cell death than activin A alone in our experiments, we hypothesised that NaB functions as a selecting reagent to ablate those cells which do not differentiate. The expression of nanog in these three treatments supported this postulation. After three days of treatment, the cells treated with activin A alone expressed the highest levels of nanog relative to cells treated with NaB alone or a combination of these treatments. These data indicate that after 3 days of activin A treatment, a subset of undifferentiated hESCs remain which account for the formation of other cell types after DMSO treatment (DMSO does not specifically direct hESCs to the definitive endoderm lineage). More recently, a three-step protocol has been developed in which a 70% hepatocyte yield was achieved [38] using activin A alone in the first stage. This difference to our results may be a consequence of the different reagents used in the second stage.

Protocols which direct hESCs down specific differentiation pathways efficiently are important for biomedical as well as regenerative medical applications. Here we report a simple and relatively economical strategy to differentiate hESCs efficiently to

hepatocytes. This system will be very useful in the further development of using hESC-derived hepatocytes for biomedical and clinical research and application.

## ACKNOWLEDGEMENTS

We thank Anish Majumdar and Jianjie Jiang from Geron Corporation for their technical help and discussion at early stage of the project; other members of the laboratories who have provided assistance through-out this project. This work was sponsored by Geron Corporation, California USA, the Biotechnology and Biological Science Research Council (BBSRC) and Institute of Obstetrics and Gynaecology Trust.

## REFERENCES

1. Thomson JA, Itskovitz-Eldor J, Shapiro SS, et al. Embryonic stem cell lines derived from human blastocysts. Science 1998;282:1145-1147

2. Reubinoff BE, Pera MF, Fong CY, et al. Embryonic stem cell lines from human blastocysts: somatic differentiation in vitro. Nat Biotechnol 2000;18:399-404

3. Soto-Gutierrez A, Kobayashi N, Rivas-Carrillo JD, et al. Reversal of mouse hepatic failure using an implanted liver-assist device containing ES cell-derived hepatocytes. Nat Biotechnol 2006;24:1412-1419

4. Rambhatla L, Chiu CP, Kundu P, et al. Generation of hepatocyte-like cells from human embryonic stem cells. Cell Transplant 2003;12:1-11

5. Lavon N, Yanuka O, Benvenisty N. Differentiation and isolation of hepatic-like cells from human embryonic stem cells. Differentiation 2004;72:230-238

6. Schwartz RE, Linehan JL, Painschab MS, et al. Defined conditions for development of functional hepatic cells from human embryonic stem cells. Stem Cells Dev 2005;14:643-655

7. Wells JM, Melton DA. Vertebrate endoderm development. Annu Rev Cell Dev Biol 1999;15:393-410

8. Tada S, Era T, Furusawa C, et al. Characterization of mesendoderm: a diverging point of the definitive endoderm and mesoderm in embryonic stem cell differentiation culture. Development 2005;132:4363-4374

9. Kubo A, Shinozaki K, Shannon JM, et al. Development of definitive endoderm from embryonic stem cells in culture. Development 2004;131:1651-1662

10. Lemaigre F, Zaret KS. Liver development update: new embryo models, cell lineage control, and morphogenesis. Curr Opin Genet Dev 2004;14:582-590

11. Gouon-Evans V, Boussemart L, Gadue P, et al. BMP-4 is required for hepatic specification of mouse embryonic stem cell-derived definitive endoderm. Nat Biotechnol 2006;24:1402-1411

12. Panduro A, Shalaby F, Shafritz DA. Changing patterns of transcriptional and post-transcriptional control of liver-specific gene expression during rat development. Genes Dev 1987;1:1172-1182

13. Spear BT. Alpha-fetoprotein gene regulation: lessons from transgenic mice. Semin Cancer Biol 1999;9:109-116

14. Tilghman SM, Belayew A. Transcriptional control of the murine albumin/alpha-fetoprotein locus during development. Proc Natl Acad Sci U S A 1982;79:5254-5257

15. Matsunaga I, Shiro Y. Peroxide-utilizing biocatalysts: structural and functional diversity of heme-containing enzymes. Curr Opin Chem Biol 2004;8:127-132

16. Hay DC, Zhao D, Ross A, et al. Direct differentiation of human embryonic stem cells to hepatocyte-like cells exhibiting functional activities. Cloning Stem Cells 2007;9:51-62

17. Xu C, Inokuma MS, Denham J, et al. Feeder-free growth of undifferentiated human embryonic stem cells. Nat Biotechnol 2001;19:971-974

18. Gerrard L, Zhao D, Clark AJ, et al. Stably transfected human embryonic stem cell clones express OCT4-specific green fluorescent protein and maintain self-renewal and pluripotency. STEM CELLS 2005;23:124-133

19. Hay DC, Sutherland L, Clark J, et al. Oct-4 knockdown induces similar patterns of endoderm and trophoblast differentiation markers in human and mouse embryonic stem cells. STEM CELLS 2004;22:225-235

20. Mitchell AM, Bridges JW, Elcombe CR. Factors influencing peroxisome proliferation in cultured rat hepatocytes. Arch Toxicol 1984;55:239-246

21. Gerrard L, Rodgers L, Cui W. Differentiation of human embryonic stem cells to neural lineages in adherent culture by blocking bone morphogenetic protein signaling. STEM CELLS 2005;23:1234-1241

22. McGrath KE, Koniski AD, Maltby KM, et al. Embryonic expression and function of the chemokine SDF-1 and its receptor, CXCR4. Dev Biol 1999;213:442-456

23. Costa RH, Grayson DR. Site-directed mutagenesis of hepatocyte nuclear factor (HNF) binding sites in the mouse transthyretin (TTR) promoter reveal synergistic interactions with its enhancer region. Nucleic Acids Res 1991;19:4139-4145

24. Schmelzer E, Zhang L, Bruce A, et al. Human hepatic stem cells from fetal and postnatal donors. J Exp Med 2007;204:1973-1987

25. Asahina K, Fujimori H, Shimizu-Saito K, et al. Expression of the liver-specific gene Cyp7a1 reveals hepatic differentiation in embryoid bodies derived from mouse embryonic stem cells. Genes Cells 2004;9:1297-1308

26. D'Amour KA, Agulnick AD, Eliazer S, et al. Efficient differentiation of human embryonic stem cells to definitive endoderm. Nat Biotechnol 2005;23:1534-1541

27. Rocken C, Licht J, Roessner A, et al. Canalicular immunostaining of aminopeptidase N (CD13) as a diagnostic marker for hepatocellular carcinoma. J Clin Pathol 2005;58:1069-1075

28. Smith JC, Price BM, Van NK, et al. Identification of a potent Xenopus mesoderm-inducing factor as a homologue of activin A. Nature 1990;345:729-731

29. Vincent SD, Dunn NR, Hayashi S, et al. Cell fate decisions within the mouse organizer are governed by graded Nodal signals. Genes Dev 2003;17:1646-1662

30. McLean AB, D'Amour KA, Jones KL, et al. Activin a efficiently specifies definitive endoderm from human embryonic stem cells only when phosphatidylinositol 3-kinase signaling is suppressed. STEM CELLS 2007;25:29-38

31. Jiang J, Au M, Lu K, et al. Generation of insulin-producing islet-like clusters from human embryonic stem cells. STEM CELLS 2007;25:1940-1953

32. Stanley LA, Horsburgh BC, Ross J, et al. PXR and CAR: nuclear receptors which play a pivotal role in drug disposition and chemical toxicity. Drug Metab Rev 2006;38:515-597

33. Bertz RJ, Granneman GR. Use of in vitro and in vivo data to estimate the likelihood of metabolic pharmacokinetic interactions. Clin Pharmacokinet 1997;32:210-258

34. Selden C, Shariat A, McCloskey P, et al. Three-dimensional in vitro cell culture leads to a marked upregulation of cell function in human hepatocyte cell lines--an important tool for the development of a bioartificial liver machine. Ann N Y Acad Sci 1999;875:353-363

35. Huang H, Hanada S, Kojima N, et al. Enhanced functional maturation of fetal porcine hepatocytes in three-dimensional poly-L-lactic acid scaffolds: a culture condition suitable for engineered liver tissues in large-scale animal studies. Cell Transplant 2006;15:799-809

36. Giuliano M, Lauricella M, Calvaruso G, et al. The apoptotic effects and synergistic interaction of sodium butyrate and MG132 in human retinoblastoma Y79 cells. Cancer Res 1999;59:5586-5595

37. Joseph J, Mudduluru G, Antony S, et al. Expression profiling of sodium butyrate (NaB)-treated cells: identification of regulation of genes related to cytokine signaling and cancer metastasis by NaB. Oncogene 2004;23:6304-6315

38. Cai J, Zhao Y, Liu Y, et al. Directed differentiation of human embryonic stem cells into functional hepatic cells. Hepatology 2007;45:1229-1239

## FIGURE LEGENDS

**Figure 1.** A three-step protocol to differentiate hESCs to hepatocytes. (**A**) Schematic representation illustrating the three-stage procedure in differentiation of hESCs to hepatocytes. (**B**) Images showing sequential morphological changes from hESCs (H7) to hepatocytes through the definitive endoderm and hepatoblast during differentiation. NaBut: sodium butyrate; DMSO: dimethyl sulfoxide; SR: knockout serum replacement; HGF: hepatocyte growth factor; OSM: oncotatin M.

**Figure 2.** Progressive alteration of the gene expression pattern during the differentiation from hESCs (H7) to hepatocytes resembles that of liver development *in vivo*. RT-PCR (**A & C**) and Western blotting (**B**) showing progressive downregulation of undifferentiated cell gene expression, transient expression of mesendoderm markers and upregulation of hepatocyte genes expression. Stages and days in differentiation are as indicated. (**D**) Flow cytometry analysis showing increase of CXCR4 expressing cells during stage 1 differentiation. ES: hES cells; F: fetal liver RNA; A: adult liver RNA. *: positive control for Pax6 from hESC-derived neural progenitor.

**Figure 3.** Characterisation of the hESCs-derived hepatocytes. (**A**) Immunocytochemistry showing expression of various markers during differentiation process. The labels on the right upper corner of each image represent day (d) and stage (st) of their differentiation and the label on the right lower corner represent antibodies used. Scale bar represents 100μm in a-d and 50μm in e & f. (**B**) Immunocytochemistry showing expression of CK18, CK19 and CD13 in hESC-

derived hepatocytes (a, b, & d respectively). Negative controls were performed with corresponding IgG and representative is shown in c. CD13 showed no staining in Hep3B cells (e). Scale bar represents 50μm.

**Figure 4.** Comparison of the effect of activin A and sodium butyrate (NaB) in the differentiation of hESCs (H7) to definitive endoderm and in the further differentiation to hepatocyte. (**A**) Phase-contrast images of hESCs treated with activin A or NaB alone or with combined activin A and NaB for three days (upper panel), then transferred to DMSO containing medium for further 4 days (lower panel). (**B**) Comparison of gene expression with these treatments during the first stage of differentiation.

**Figure 5**. Functional test of hESC-derived hepatocytes. (**A**) hESC-derived hepatocytes produce and secrete plasma proteins, fibrinogen, fibronectin and alpha-2 macroglobulin, which are significant higher in comparison to their original hESCs, * and ** representing $P<0.005$ and $P<0.01$ by student t test. (**B**) hESC-derived hepatocytes express cytochrome p450 reductase (CPR), CYP3A of P450 family and c-met. They also exhibit evident glycogen storage. Scale bar represent 100μm in glycogen and 50μm in the rest.

**Figure 6.** Cytochrome p450 isozymes in hESC-derived hepatocytes (hESC-HC). (**A**) Western blotting showing protein expression of CYP3A (CYP3A4, CYP3A5, CYP3A7) and CYP2D6 in hESCs and hESC-HC from 2 experiments. (**B**) RT-PCR showing CYP3A4, CYP3A7 and CYP2C9 and CYP2C19 expression in hESC, hESC-derived definitive endoderm (DE, end of stage 1), hESC-derived hepatocytes (hESC-

HC), fetal and adult liver. (**C**). Basal metabolism of p450 substrates. The p450 substrates as indicated were administered to the cells and their metabolites were detected by mass spectrometry and normalised over alanine aminotransferase (ALT). The p values were calculated by student *t* test between HepG2 cells and hESC-HC. (**D**). Induction of CYP3A4 by rifampicin in both hESC-HC and HepG2 cells. The cells were treated with rifampicin or vehicle, DMSO, for 72 hours prior CYP3A4 substrate midazolam administration. The metabolite 1'hydroxymidazolam (1'OH-Midazolam) was measured by mass spectrometry and normalised over alanine aminotransferase (ALT). The p value was calculated in hESC-HC by student *t* test between control (DMSO) and rifampicin treatment.

## SUPPLEMENTAL FIGURE LEGENDS

**Figure 7.** (**A**) High magnification image of hESC-derived hepatocytes. (**B**) hESC-derived hepatocytes in culture at day 24 of differentiation showing deteriorated hepatocytes with increased fiber-producing cells. (**C**) Periodic Acid Schiff (PAS) staining on fibroblast cells showing no glycogen storage.

**Figure 8.** Differentiation of H1 hESC line showing a similar gene expression pattern to H7. (**A** & **B**). Gene expression profile of H1 during differentiation (A) and at the first stage of differentiation with activin or NaBut alone or with combined treatment (B). (**C**). Generation and secretion of plasma protein in H1 cells.

**Figure 9.** RT-PCR showing CYP7A1 expression in hESC, hESC-derived hepatocytes (hESC-HC) and fetal and adult liver tissues.

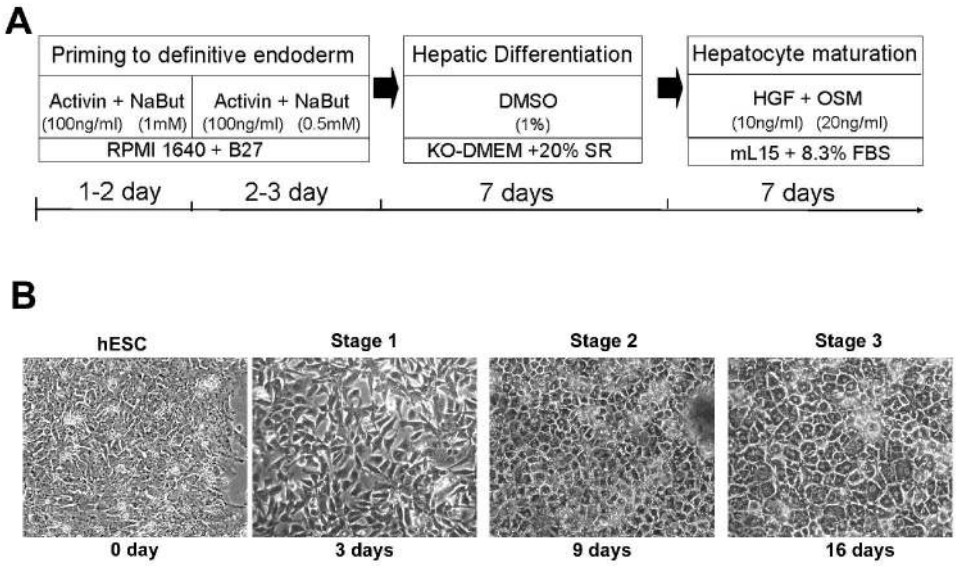


111x68mm (600 x 600 DPI)

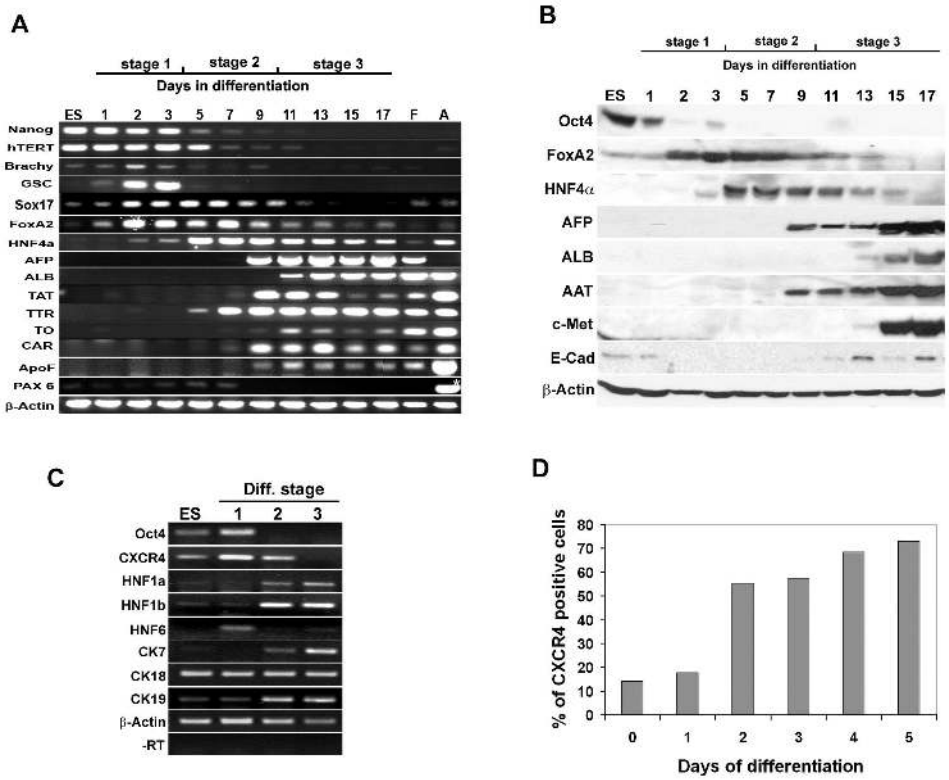


167x139mm (300 x 300 DPI)

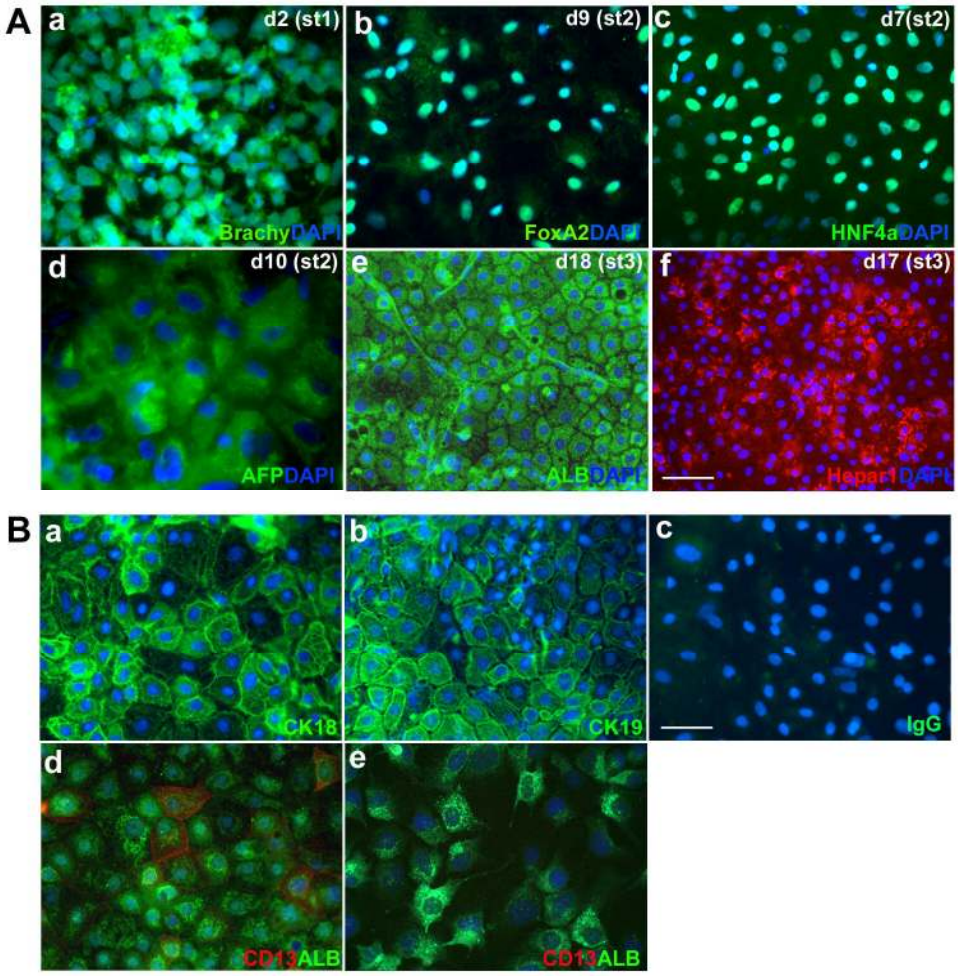


198x195mm (300 x 300 DPI)

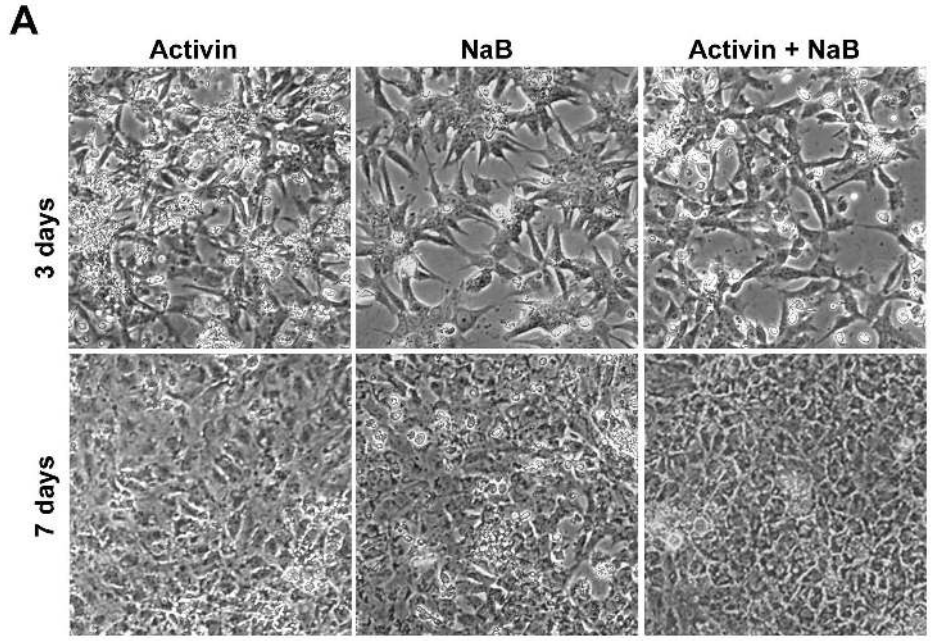


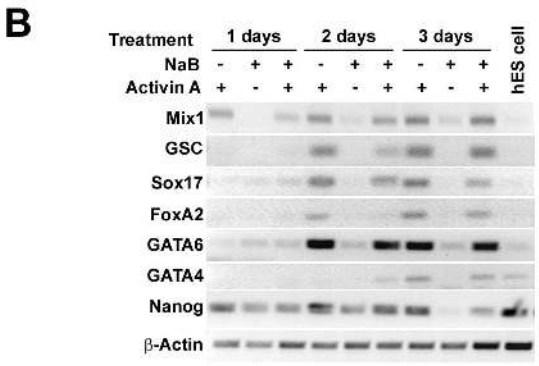


160x187mm (300 x 300 DPI)

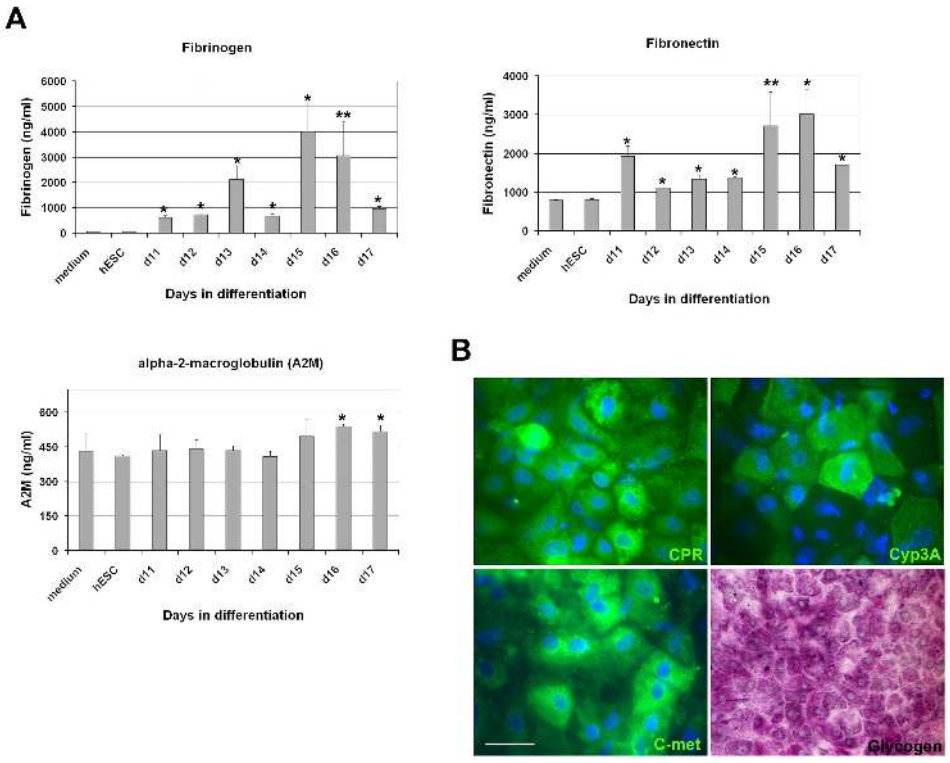


209x172mm (300 x 300 DPI)

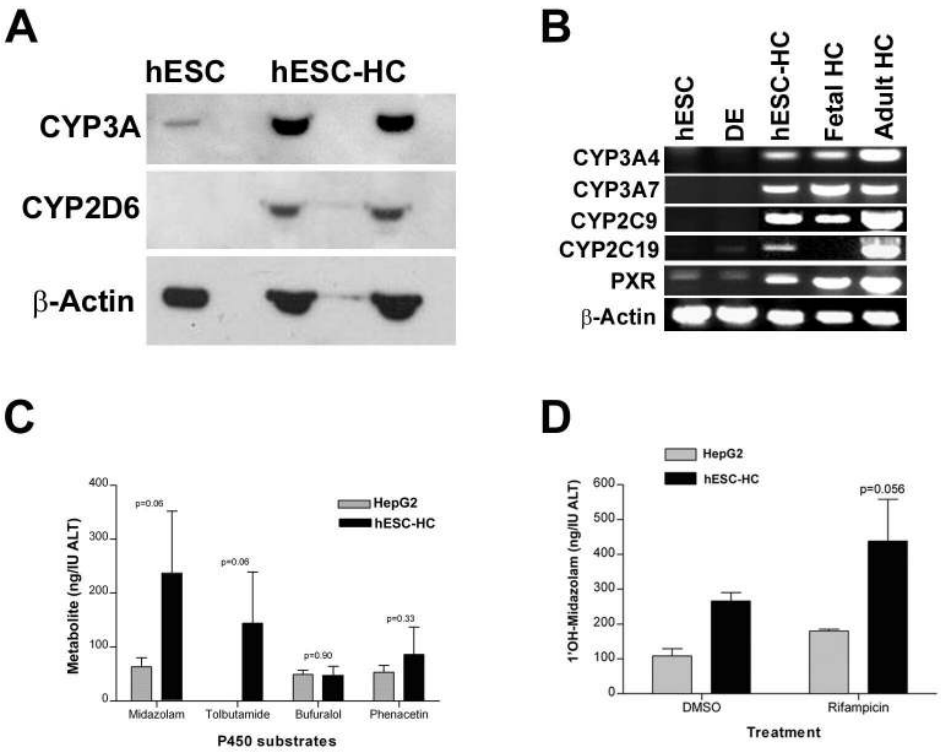


138x115mm (300 x 300 DPI)

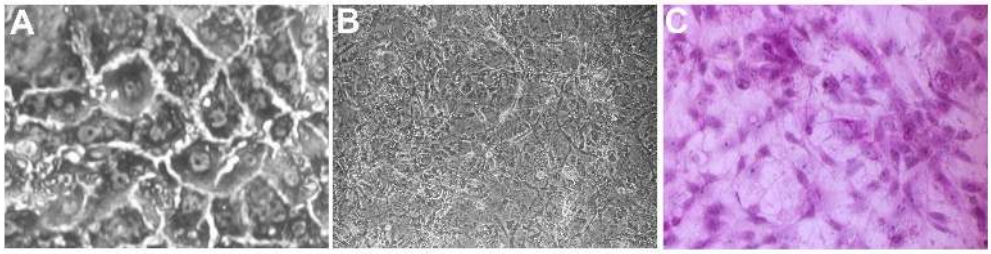


185x47mm (300 x 300 DPI)

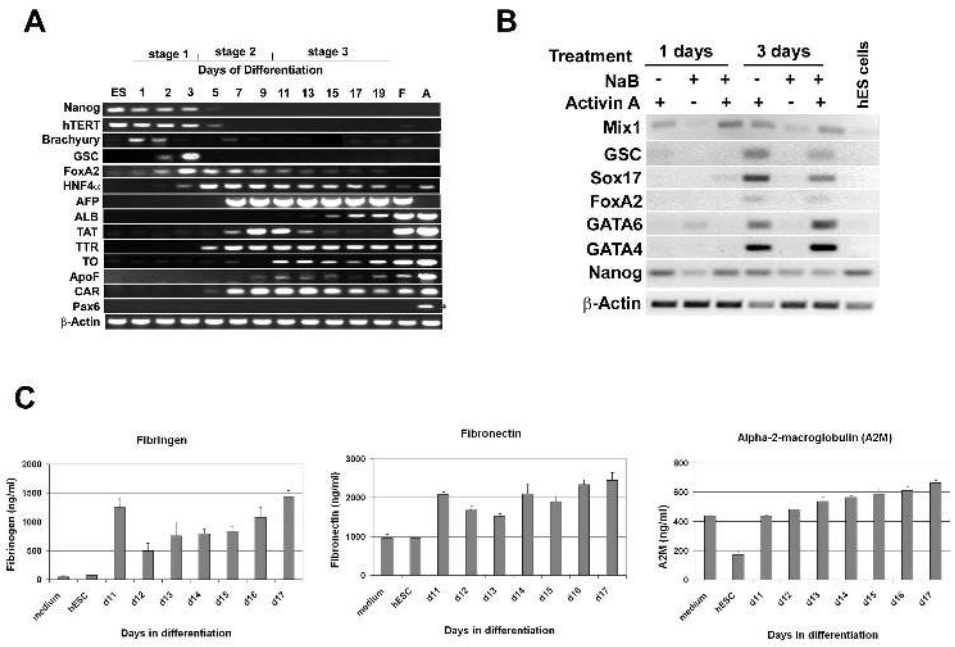


206x148mm (300 x 300 DPI)

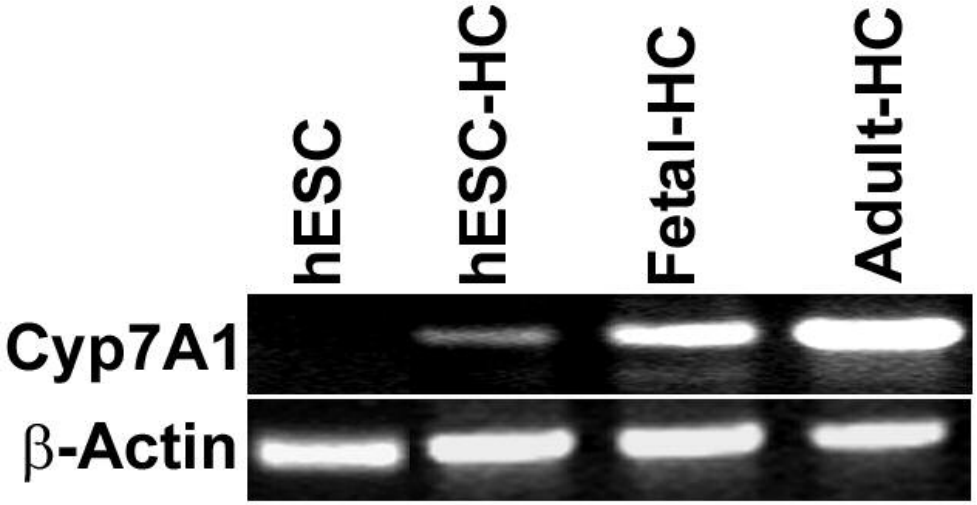


54x29mm (300 x 300 DPI)

## Suppl. Table 1. PCR primers and conditions

| Name | Forward primer (5'-3') | Reverse primer (5'-3') | size | Ta (°C) |
|---|---|---|---|---|
| AFP | AGAACCTGTCACAAGCTGTG | GACAGCAAGCTGAGGATGTC | 675 bp | 55 |
| ALB | CCTTTGGCACAATGAAGTGGGTAACC | CAGCAGTCAGCCATTTCACCATAGG | 354 bp | 55 |
| ApoF | GGAAGCGATCAAACCTACCA | ATCAGCCTGACAACCAGCTT | 347 bp | 55 |
| β-Actin | TCACCACCACGGCCGAGCG | TCTCCTTCTGCATCCTGTCG | 350 bp | 61 |
| Brachyury | GTGACCAAGAACGGCAGGAGG | TGTTCCGATGAGCATAGGGGC | 706 bp | 61 |
| CAR | CAGCAAACACCTGTGCAACTG | AAGGGCTGGTGATGGATGAA | 145 bp | 57 |
| CK7 | TCGCTGAGGTCAAGGCACAG | CACTCCTCAGCCTCGGCAAT | 241 bp | 59 |
| CK18 | GGGCCCAATATGACGAGCTG | AGCAGGATCCCGTTGAGCTG | 270 bp | 59 |
| CK19 | CTCCCGCGACTACAGCCACT | TCAGCTCATCCAGCACCCTG | 211bp | 59 |
| CXCR4 | CACCGCATCTGGAGAACCA | GCCCATTTCCTCGGTGTAGTT | 79 bp | 55 |
| Cyp2C19 | ATGTTTGCTTCTCCTTTCAA | CCAAAATATCACTTTCCATAA | 700 bp | 49 |
| Cyp2C9 | ACATTGACCTTCTCCCCACCAGCC | CAAATCCATTGACAACTGGAGTGG | 356 bp | 57 |
| Cyp3A4 | CCTTACATATACACACCCTTTG | GGTTGAAGAAGTCCTCCTAAGCT | 169 bp | 50 |
| Cyp3A7 | CTATGATACTGTGCTACAGT | TCAGGCTCCACTTACGGTCT | 455 bp | 50 |
| Cyp7A1 | GTGCCAATCCTCTTGAGTTCC | ACTCGGTAGCAGAAAGAATACATC | 397 bp | 55 |
| FOXA2 | AGATGGAAGGGCACGAGC | CAGGCCGGCGTTCATGTT | 88 bp | 56 |
| GATA4 | CATCAAGACGGAGCCTGGCC | TGACTGTCGGCCAAGACCAG | 218 bp | 60 |

| | | | | |
|---|---|---|---|---|
| GATA6 | CCATGACTCCAACTTCCACC | ACGGAGGACGTGACTTCGGC | 213 bp | 57 |
| GSC | GAGGAGAAAGTGGAGGTCTGGTT | CTCTGATGAGGACCGCTTCTG | 71 bp | 61 |
| HNF1α | TACACCACTCTGGCAGCCACACT | CGGTGGGTACATTGGTGACAGAAC | 114 bp | 59 |
| HNF1β | TCACAGATACCAGCAGCATCAGT | GGGCATCACCAGGCTTGTA | 79 bp | 55 |
| HNF4α | CTGCTCGGAGCCACCAAGAGATCCATG | ATCATCTGCCACGTGATGCTCTGCA | 370 bp | 55 |
| HNF6 | CGCTCCGCTTAGCAGCAT | GTGTTGCCTCTATCCTTCCCAT | 61 bp | 55 |
| Mix1 | GGTACCCCGACATCCACTT | GCCTGTTCTGGAACCATACCT | 87 bp | 57 |
| Nanog | AGCCTCTACTCTTCCTACCACC | TCCAAAGCAGCCTCCAAGTC | 278 bp | 60 |
| Oct4 | GACAACAATGAAAATCTTCAGGAGA | TTCTGGCGCCGGTTACAGAACCA | 218 bp | 60 |
| Pax6 | AACAGACACAGCCCTCACAAACA | CGGGAACTTGAACTGGAACTGAC | 275 bp | 60 |
| PXR | GGAGAAGTCGGAGCAAAGAA | AGCTCCCTGATCATCATCCGC | 517 bp | 58 |
| SOX17 | CCAGAATCCAGACCTGCACAA | CTCTGCCTCCTCCACGAA | 100 bp | 57 |
| TAT | ACTGTGTTTGGAAACCTGCC | GCAGCCACTTGTCAGAATGA | 188 bp | 55 |
| TERT | AGC GAC TAC TCC AGC TAT G | GTT CTT GGC TTT CAG GAT GG | 304 bp | 61 |
| TO | GGCAGCGAAGAAGACAAATC | TCGAACAGAATCCAACTCCC | 218 bp | 55 |
| TTR | GCCGTGCATGTGTTCAGAAAG | GACAGCCGTGGTGGAATAGGA | 258 bp | 58 |

## Suppl. Table 2. List of antibodies used.

**Primary antibodies**

| Antigen | Type | Company | Dilution |
|---|---|---|---|
| AAT | Mouse Mono | QED Bioscience | 1/2000 (WB) |
| AFP | Mouse Mono | SIGMA | 1/2000 (WB); 1/500 (ICC) |
| ALB | Mouse Mono | SIGMA | 1/2000 (WB); 1/500 (ICC) |
| β-Actin | Mouse Mono | SIGMA | 1/10000 (WB) |
| Brachyury | Goat Poly | R and D Systems | 1/20 (ICC) |
| CD13 | Mouse Mono | Invitrogen | 1/50 (ICC) |
| CK18 | Mouse Mono | Invitrogen | 1/50 (ICC) |
| CK19 | Mouse Mono | Invitrogen | Ready made |
| C-MET | Rabbit Poly | Santa Cruz | 1/100 (WB); 1/25 (ICC) |
| CPR | Rabbit Poly | ABCAM | 1/500 (ICC) |
| CXCR4 - PE | Mouse Mono | R and D Systems | 1:3.5 |
| CYP3A | Sheep poly | U. of Dundee | 1/1000 |
| CYP2D6 | Sheep poly | U. of Dundee | 1/1000 |
| E-CAD | Mouse Mono | DAKO | 1/100 (WB) |
| FOXA2 | Goat Poly | R and D Systems | 1/200 (WB); 1:20 (ICC) |
| HEPPAR1 | Mouse Mono | DAKO | 1/25 (ICC) |
| HNF4a | Rabbit Poly | Santa Cruz | 1/200 (WB); 1/100 (ICC) |
| OCT-4 | Mouse Mono | Santa Cruz | 1/200 (WB) |

| Secondary antibodies | | |
|---|---|---|
| **Type** | **Company** | **Dilution** |
| Goat anti –mouse IgG HRP | DAKO | 1/2,500 |
| Goat anti-rabbit IgG HRP | DAKO | 1/2,500 |
| Rabbit anti goat IgG HRP | DAKO | 1/2,500 |
| Goat anti-sheep | Santa Cruz | 1/2,500 |
| Alexa Fluor 488 goat anti-mouse | Molecular Probes | 1/500 |
| Alexa Fluor 488 goat anti-rabbit | Molecular Probes | 1/500 |
| Alexa Fluor 568 goat anti-mouse | Molecular Probes | 1/500 |
| Alexa Fluor 488 donkey anti-goat | Molecular Probes | 1/500 |
| Alexa Fluor 488 donkey anti-sheep | Molecular Probes | 1/500 |